JCB Report

An Inducible Mouse Model for Epidermolysis Bullosa Simplex: Implications for Gene Therapy

Tongyu Cao,* Mary Ann Longley,* Xiao-Jing Wang,*‡ and Dennis R. Roop*‡

*Department of Molecular and Cellular Biology and ‡Department of Dermatology, Baylor College of Medicine, Houston, Texas 77030

Abstract. The Dowling-Meara variant of epidermolysis bullosa simplex (EBS-DM) is a severe blistering disease inherited in an autosomal-dominant fashion. Here we report the generation of a mouse model that allows focal activation of a mutant keratin 14 allele in epidermal stem cells upon topical administration of an inducer, resulting in EBS phenotypes in treated areas. Using laser capture microdissection, we show that induced blisters healed by migration of surrounding nonphenotypic stem cells into the wound bed. This observation provides an explanation for the lack of mosaic forms of EBS-DM. In addition, we show that decreased mutant keratin 14 expression resulted in normal morphology and functions of the skin. Our results have important implications for gene therapy of EBS and other dominantly inherited diseases.

Key words: epidermolysis bullosa simplex • gene therapy • gene targeting • epidermal stem cells • keratins

Introduction

The primary function of the epidermis is to provide a protective barrier for the internal tissues and organs. The structural integrity of epidermal keratinocytes is maintained by a filamentous network made up of keratins, which belong to the intermediate filament (IF)[1] protein superfamily (Moll et al., 1982; Quinlan et al., 1985). Two types of keratin subunits have been described. In general, type I keratin subunits are smaller, with an acidic pI, and are encoded by genes located on chromosome 17 (Quinlan et al., 1985). Type II keratin subunits are larger and more basic, and are encoded by genes located on chromosome 12 (Quinlan et al., 1985).

The basic structure of keratins is an α-helical rod domain made up of repeating units of seven amino acids. One member of each type of keratins is needed to form a heterodimer through the rod domain, which then assembles into higher order structures to form mature keratin filaments (Hatzfeld and Weber, 1990; Steinert, 1990; Rothnagel and Roop, 1995). The α-helical rod domain is not continuous but is made up of four helical segments, termed 1A, 1B, 2A, and 2B (Steinert and Roop, 1988). The beginning of 1A and the end of 2B overlap with the neighboring keratin molecules and are crucial for the stability of the keratin filaments (Rothnagel and Roop, 1995). Mutations in these regions of keratin genes have been identified in patients with epidermolysis bullosa simplex (EBS) and epidermolytic hyperkeratosis (EHK) (Rothnagel and Roop, 1995).

The Dowling-Meara variant of EBS (EBS-DM, or EB Herpetiformis, MIM No. 131760) is the most severe form of EBS, and it is inherited in an autosomal-dominant fashion. At birth, it presents with generalized blisters in areas prone to mechanical trauma (Dowling and Meara, 1954; Marinkovich et al., 1999). The underlying mechanism of basal cell lysis is the disintegration of the IF network and the formation of perinuclear keratin clumps (Anton-Lamprecht and Schnyder, 1982; McGrath et al., 1992). EBS-DM has been linked to chromosomes 12 and 17, and mutations in keratin 5 (K5) and keratin 14 (K14) genes expressed in basal keratinocytes have been identified in these patients (Letai et al., 1993; Chen et al., 1995; Rothnagel and Roop, 1995). In addition, a mutational "hot spot" at codon 125 resulting in the change of an arginine in the 1A region of the K14 rod domain was found in 70% of EBS-DM patients (Rothnagel and Roop, 1995).

Two mouse models were previously generated for EBS (Vassar et al., 1991; Lloyd et al., 1995). Both exhibited

Address correspondence to Dennis R. Roop, Ph.D., Department of Molecular and Cellular Biology, Baylor College of Medicine, One Baylor Plaza, Houston, TX 77030. Tel.: (713)798-4966. Fax: (713)798-3800. E-mail: roopd@bcm.tmc.edu

[1]*Abbreviations used in this paper:* EBS, epidermolysis bullosa simplex; EBS-DM, Dowling-Meara variant of EBS; ES, embryonic stem; EHK, epidermolytic hyperkeratosis; IF, intermediate filament; neo, neomycin.

EBS-like phenotypes, but neither mimicked the dominantly inherited disease at the genetic level. To test gene therapy approaches for EBS, it is necessary to generate a mouse model that mimics EBS at both the genetic and phenotypic levels. In this study, we generated a mouse model that fulfills these criteria. To elucidate the involvement of epidermal stem cells, we also developed a mouse model that allowed focal induction of EBS phenotypes.

Materials and Methods

Construction of the Targeting Vector

A genomic clone containing the mouse K14 gene in bacterial phage P1 was isolated from a 129/SVJ genomic library (Incyte Genomics). A C→T point mutation at codon 131 (resulting in an arginine to cysteine substitution) in mouse K14 was engineered in a 1.3-kb BamHI fragment by PCR, which was then used to replace the wild-type BamHI fragment in the gene. For the selection of recombinant embryonic stem (ES) cells, a neomycin-resistance (neo) cassette flanked by loxP sites (a gift from R.R. Behringer and Y. Mishina, University of Texas, M.D. Anderson Cancer Center, Houston, TX) was inserted into the PmlI site in intron I of the mutant K14 gene. This insertion also introduced an EcoRV restriction site that allowed us to identify homologous recombination by Southern blot analysis.

Generation of mtK14^{neo} and mtK14^{loxP} Mice

Mouse 129/SVJ ES cells (Incyte Genomics) were electroporated with the linearized targeting vector, and homologous recombination in ES cell clones was identified by Southern blot analysis of genomic DNA digested with Eco RV. The presence of the C→T mutation was confirmed by sequence analysis. Recombinant ES cells (mtK14^{neo}) were injected into C57BL/6 blastocysts. Three independent mtK14^{neo} mouse lines were generated, and were phenotypically indistinguishable. The mtK14^{neo} ES cells were also transfected with a CMV-Cre plasmid (a gift from S. O'Gorman, The Salk Institute for Biological Studies, San Diego, CA), and cells without the neo cassette (mtK14^{loxP}) were injected into blastocysts as well.

RNA Preparation and Semi-quantitative RT-PCR Analysis

Total RNA from newborn pup epidermis was isolated using RNAzol B (Tel-Test). Equal amounts of total RNA from epidermal samples were reverse transcribed into cDNA. The cDNA was amplified by semi-quantitative PCR using K14-specific primers: 5′-CTAGCCGCATGTCCTCCATC-3′ and 5′-biotin-CCGAATCTTCACCTCCAGTTC-3′. PCR products were gel purified and digested with AciI (New England Biolabs, Inc.). Digestion of the wild-type PCR products yielded a 71-bp biotinylated fragment. The C→T mutation destroyed an AciI site, resulting in a 136-bp biotinylated fragment from the mutant PCR products. Digested DNA fragments were separated by gel electrophoresis, blotted onto GeneScreenPlus membrane (New England Biolabs, Inc.), and detected with BrightStar BioDetect kit (Ambion). The intensity of the signals was determined by QuantiScan software (Biosoft).

Immunofluorescence Microscopy and Transmission Electron Microscopy

Biopsied skin was fixed in 10% Formalin (Fisher Scientific) or embedded in OCT (Sakura Finetek USA), and indirect immunofluorescent staining of sections was performed as previously described (Wojcik et al., 2000), using a guinea pig anti-K14 antibody, a rabbit anti-K10 antibody, a rabbit anti-loricrin antibody, and a rat anti-integrin α6 antibody (Chemicon) (Wang et al., 1995). The anti-K14 antibody recognized both wild-type and mutant mouse K14. Transmission electron microscopy was carried out following standard protocol (Wang et al., 1995).

Laser Capture Microdissection

Biopsied skin from healed blistered area on the palm of RU486 treated mtK14^{neo}/CrePR1 pups was fixed in 10% Formalin and embedded in paraffin (Wojcik et al., 2000). Paraffin slides were stained with Nuclear Fast Red (Vector Laboratories), and epidermal cells under the scab were transferred onto a thermoplastic polymer film (CapSure™) by a near infrared laser pulse on a PixCell I microscope/laser capture equipment (Arcturus Engineering). Genomic DNA was extracted from cells attached to the film in 10 mM Tris-HCl (pH 8.0), 0.2 mM EDTA (pH 8.0), 0.25% Tween 20, and 0.5% Nonidet P-40 containing 1 mg/ml proteinase K. DNA was then analyzed by PCR. For the presence of the loxP site, primers 5′-GAACTGGAGGTGAAGATTCG-3′ (in exon I of K14) and 5′-GGGTTATTGAATATGATCGG-3′ (in the loxP site) were used. For the presence of the neo cassette, primers 5′-GCGGAACCCTTAATATAACT-3′ (in the linker region of the neo cassette) and 5′-CCACACAGTCAGCTTCAACC-3′ (in intron I of K14) were used.

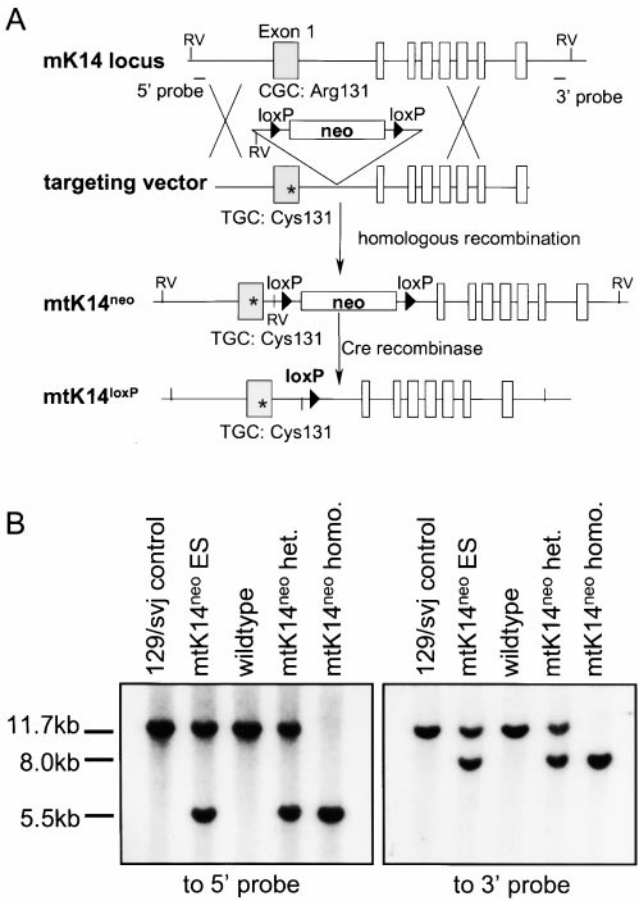

Figure 1. Targeting strategy and Southern blot analysis. (A) Targeting strategy. Open boxes represent the exons. The asterisk denotes the C→T point mutation, and neo denotes the neomycin-resistance selection cassette. (B) Southern blot analysis of EcoRV-digested genomic DNA. The 5′ external probe (A) hybridized to an 11.7-kb fragment from the wild-type K14 locus, and a 5.5-kb fragment from the mtK14^{neo} locus. The 3′ external probe (A) hybridized to the same 11.7-kb fragment from the wild-type K14 locus, and an 8.0-kb fragment from the mtK14^{neo} locus. het., heterozygote; homo., homozygote.

Results and Discussion

Characterization of mtK14^{neo} Mice

To generate a mouse model that mimics EBS-DM at the genetic level, we introduced a point mutation in codon 131 (equivalent to arginine 125 in human K14) of the mouse K14 gene. The gene targeting vector used to introduce this mutation into ES cells also contained a neo cassette in intron I (Fig. 1 A). The linearized targeting vector was elec-

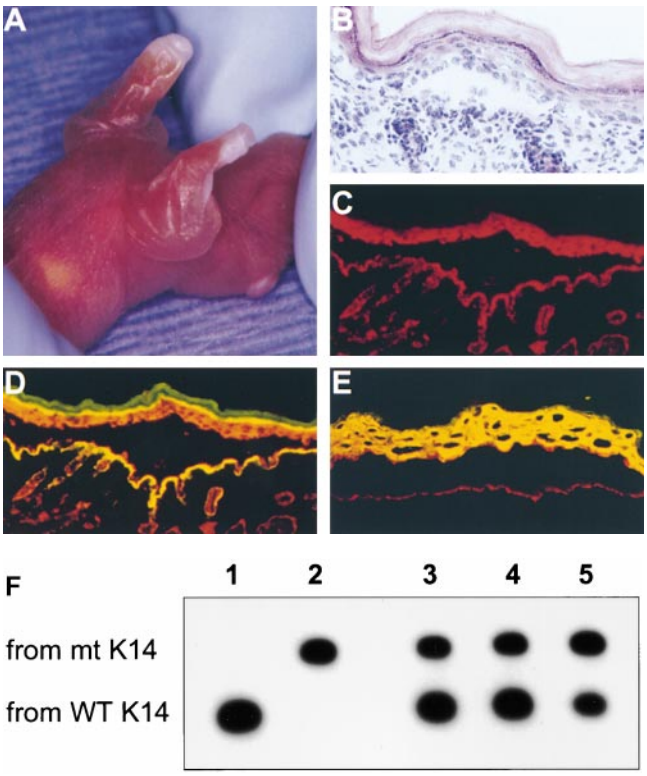

Figure 2. Phenotype of homozygous mtK14^{neo} pups. (A) Gross phenotype of a 1-d-old pup, showing severe blisters on the front legs, paws, and chest. (B) H&E staining of skin from a homozygous mtK14^{neo} pup. The separation occurred in the basal cell layer within the epidermis. (C–E) Immunofluorescence microscopy of pup skin. The sections were stained for mutant K14 (Texas red, C–E), integrin α6 (FITC, D), and keratin 10 (FITC, E). Overlapping of K14 staining with either integrin α6 (D) or keratin 10 (E) results in yellow fluorescence. (F) AciI digestion of semi-quantitative RT-PCR products from mouse RNA. (1) Wild type; (2) homozygous mtK14^{neo}; (3 and 4) +/mtK14^{neo}; (5) +/mtK14^{loxP}. Note the lower expression levels of mtK14^{neo} allele in +/mtK14^{neo} mice shown in lanes 3 and 4.

troporated into ES cells, and homologous recombination was identified by Southern blot analysis of genomic DNA from these cells (Fig. 1 B). The presence of the point mutation was confirmed by sequence analysis (data not shown).

Correctly targeted ES cells bearing the point mutation were injected into mouse blastocysts, and heterozygous mtK14^{neo} (+/mtK14^{neo}) mice were derived. These mice appeared normal with no gross skin phenotypes, and histological analysis did not show microscopic blisters (data not shown). This was unexpected as the equivalent mutation in humans results in a dominantly inherited disease. We hypothesized that the lack of a phenotype in these mice was due to an interference of the neo cassette with the expression of the mutant K14 gene. This hypothesis was supported by semi-quantitative RT-PCR analysis that showed a twofold lower expression of mtK14^{neo} than wild-type K14 (Fig. 2 F).

Homozygous mtK14^{neo} pups were normal at birth. However, within hours after birth, they developed extensive blisters on the front legs, paws, and chest (Fig. 2 A), and usually died within 48 h. Histological analysis indicated a separation within the basal cell layer of the epidermis (Fig. 2 B), which was confirmed by indirect immunofluorescent staining of K14 and integrin α6, showing an intact basement membrane (Fig. 2, C and D). These results suggest that the separation occurred due to cytolysis of basal keratinocytes. Immunofluorescence microscopy using various differentiation markers such as keratin 10 (Fig. 2 E) and loricrin (data not shown) did not indicate any changes in the differentiation of the epidermis. Transmission electron microscopy revealed keratin clumps in the basal keratinocytes of lesional areas (data not shown). Primary keratinocytes isolated from homozygous mtK14^{neo} pups showed a collapsed perinuclear IF network and cytoplasmic keratin aggregates when subjected to heat shock, whereas a normal IF network remained in wild-type keratinocytes under identical conditions (data not shown). These results are consistent with observations made in EBS-DM patients and their cultured keratinocytes (Coulombe, 1993; Morley et al., 1995; Marinkovich et al., 1999).

Like the previously reported K14 null mice (Lloyd et al., 1995), the homozygous mtK14^{neo} pups resembled a recessive form of EBS (Chan et al., 1994; Rugg et al., 1994; Jonkman et al., 1996). However, the homozygous mtK14^{neo} pups exhibited a more severe phenotype. Although some K14 null mice lived for as long as 3 mo presumably due to functional compensation by keratin 15 (Lloyd et al., 1995), more than 95% of the homozygous mtK14^{neo} pups died within 48 h after birth, and none lived beyond 5 d. This more severe phenotype is likely due to the significant amount of mutant K14 in these mice (Fig. 2, C and F). We suspect that mutant K14 competed with the low level of keratin 15 in newborn pups for dimerization with K5, resulting in the absence of functional keratin filaments in the basal layer.

Characterization of mtK14^{loxP} Mice

To unequivocally demonstrate that the low expression level of the mutant K14 allele led to the absence of a phenotype in +/mtK14^{neo} mice, we deleted the neo cassette in mtK14^{neo} ES cell clones via Cre-mediated excision (Fig. 1 A). Heterozygous mtK14^{loxP} (+/mtK14^{loxP}) pups derived from these ES cells spontaneously developed large blisters on their forelimbs and trunk (Fig. 3 A), as expected for this dominant mutation. Semi-quantitative RT-PCR analysis of RNA isolated from these pups showed comparable expression levels of the mutant and wild-type K14 alleles (Fig. 2 F). Histological analysis and immunofluorescence microscopy revealed similar findings as in the homozygous mtK14^{neo} pups (data not shown).

An important diagnostic feature of EBS-DM is the collapsed IF filaments revealed upon ultrastructural examination (Anton-Lamprecht and Schnyder, 1982; Marinkovich et al., 1999). Transmission electron microscopy showed keratin clumps in the basal keratinocytes of +/mtK14^{loxP} pups (Fig. 3, B, E, and F). Short IF filaments were also observed in basal keratinocytes (Fig. 3, E and G), probably due to the significant amount of wild-type K14. In contrast, long IF filaments were observed in the basal keratinocytes in wild-type littermates (Fig. 3 D). The keratin clumps and short filaments were sometimes attached to desmosomes or hemidesmosomes, or in the perinuclear space (Fig. 3,

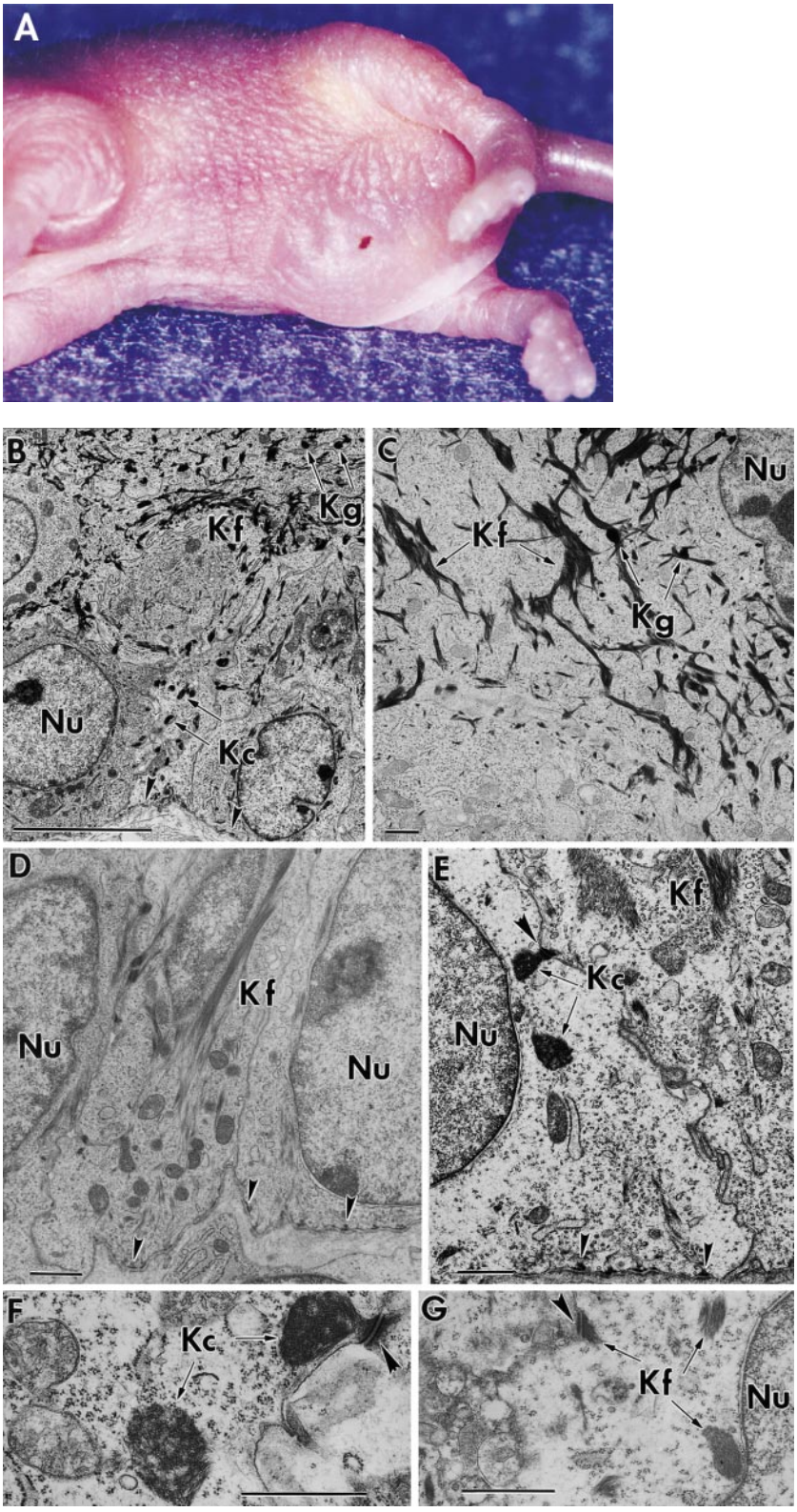

Figure 3. Phenotype of +/mtK14^{loxP} pups. (A) Gross phenotype of a 2-d-old pup, showing blisters on the left front leg and abdomen. (B–G) Transmission electron microscopy of skin samples from +/mtK14^{loxP} pups (B, C, and E–G) and normal littermate (D). The mtK14^{loxP} pup skin showed keratin clumps and short keratin filaments in the basal keratinocytes (B, E–G), but normal keratin filaments in the suprabasal layer of the epidermis (B and C). Normal skin showed long keratin filaments in the basal keratinocytes (D). Kc, keratin clumps; Kf, keratin filaments; Kg, keratohyalin granules; Nu, nucleus. Small arrowheads denote hemidesmosomes, indicating the position of the basement membrane. Large arrowheads denote desmosomes. Bars: (B) 5 μm; (C) 100 nm; (D–G) 1 μm.

E–G). Some basal cells of the mutant were vacuolated, and in the blistering areas, lymphocyte infiltration was observed (data not shown). The suprabasal keratinocytes appeared normal, with abundant keratin bundles and desmosomes in the spinous and granular cells (Fig. 3 C). Unfortunately, +/mtK14^{loxP} pups died within a week after birth due to severe blistering.

An Inducible Mouse Model for EBS

It is important to note that although +/mtK14^{neo} pups appeared normal, +/mtK14^{loxP} pups with increased mutant K14 expression developed severe EBS-like phenotypes. These observations suggested that we might be able to generate a viable model for EBS if we could focally delete the neo cassette in +/mtK14^{neo} mice.

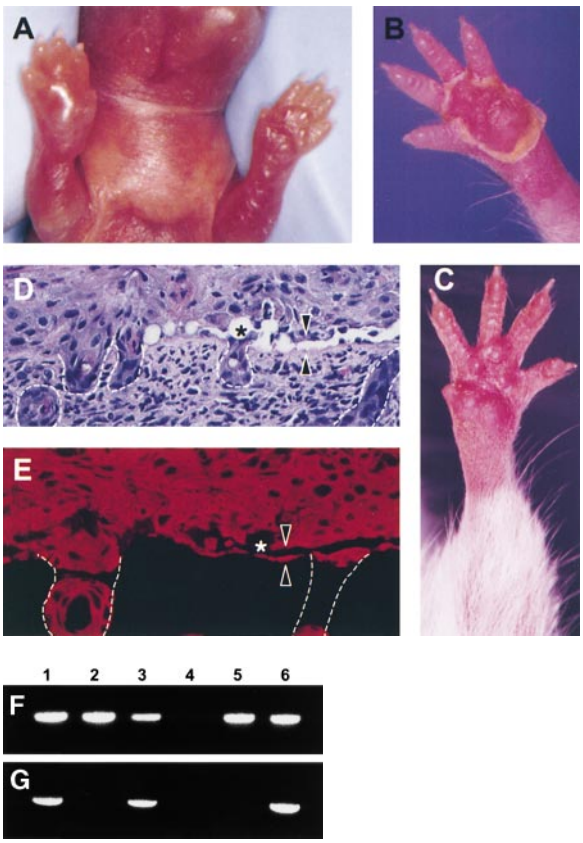

Figure 4. Induction and characterization of RU486 induced blisters. (A) Gross phenotype of an induced blister on a mtK14^{neo}/CrePR1 pup after two RU486 treatments on the right front leg. No blisters developed on the untreated leg (A) or in +/mtK14^{neo} or CrePR1 control pups treated with RU486 (data not shown). (B) The right front paw of a mtK14^{neo}/CrePR1 pup 10 d after blister formation upon treatment. (C) The left front paw and leg of a mtK14^{neo}/CrePR1 mouse 6 mo after blister formation and cessation of RU486 treatment. The blistered area, including the palm and leg, healed without scarring, and there is normal hair growth on the leg. No additional blisters formed without further RU486 treatment. (D and E) H&E staining (D) and immunofluorescence microscopy with an anti-K14 antibody (Texas red, E) of an induced blister edge. Blistering occurred in the basal keratinocytes (arrowheads) on the chest (D and E), front leg, and paw (data not shown). The asterisk denotes cytolysis, and dashed lines outline the hair follicles. (F and G) PCR analysis of DNA for the presence of the loxP site (F) and neo cassette (G). (1–3) Epidermal DNA samples from different areas of a treated mtK14^{neo}/CrePR1 pup. (1) Untreated area; (2) blister roof; (3) healed blistered area 1 wk after blister formation. (4–6) DNA samples from control mice. (4) Wild type; (5) +/mtK14^{loxP}; (6) +/mtK14^{neo}.

To achieve this goal, we exploited a recently developed transgenic mouse model that allows focal deletion of genomic sequences upon topical application of an inducer (Berton et al., 2000). This system uses tissue-specific expression of Cre-recombinase fused to a truncated progesterone receptor (PR1) (Kellendonk et al., 1996) under the control of an epithelial-specific promoter, such as that of K5 or K14 (Berton et al., 2000). PR1 does not bind to endogenous progesterone, but binds to antiprogestin (Kellendonk et al., 1996). In the absence of an antiprogestin, the CrePR1 fusion protein is expressed in the basal keratinocytes and hair follicles, but is retained in the cytoplasm and remains inactive. Upon topical administration of an antiprogestin, such as RU486, CrePR1 translocates to the nucleus and becomes active.

Mice carrying the CrePR1 transgene under the control of a K5 or K14 promoter were bred with +/mtK14^{neo} mice, and bigenic pups (mtK14^{neo}/CrePR1) were obtained. RU486 (0.5 mg/ml in ethanol) was applied once daily to the forelimbs and chest of newborn pups, areas prone to mechanical trauma. After several (two to seven) days of RU486 treatment, we observed blisters filled with fluid on the front legs and paws of bigenic pups (Fig. 4 A). RU486 treatment was terminated once blisters became visible. Histological analysis and immunofluorescence microscopy revealed that blistering occurred within the basal layer of the epidermis, as expected (Fig. 4, D and E).

PCR analysis of DNA isolated from keratinocytes in the blister roof revealed the presence of the loxP site, but not the neo cassette (Fig. 4, F and G). This result indicates that activation of the CrePR1 fusion protein and the subsequent excision of the neo cassette can be efficiently achieved with as few as two RU486 treatments. Upon termination of RU486 treatment, the induced blistered areas healed without scarring in 2 wk (Fig. 4, B and C). No additional blisters formed without further RU486 treatment. When we dissected the healed area 1 wk after blister formation and extracted DNA from epidermal cells under the scab, isolated by laser capture microdissection, the presence of the neo cassette was detected (Fig. 4 G).

It is possible that CrePR1 was only activated in the nonstem cell population of basal keratinocytes (transit amplifying cells) in the blistered area. Although blisters were induced through cytolysis of these cells, the stem cells were not targeted, i.e., they retained the neo cassette and repopulated the area after 7 d. However, this is not likely the case based on observations in the accompanying manuscript (Arin et al., 2001), where the same inducible system was used to develop a mouse model for EHK. In the EHK mouse model, lesions develop in the suprabasal keratinocytes although the basal cells (including the stem cells) remain normal. Unlike our EBS lesions, induced EHK lesions persist, to date for 6 mo. Because the normal turnover time for mouse epidermis is ~8–10 d (Potten et al., 1987), this result clearly shows that epidermal stem cells are targeted by our inducible system. Therefore, the presence of mtK14^{neo} allele in the healed area is best explained by migration and reepithelialization by nonphenotypic mtK14^{neo} stem cells or transit amplifying cells derived from these stem cells from the untreated surrounding area. Healing of the induced blisters and the absence of recurrent lesions have significant implications for gene therapy of EBS, as defective stem cells may be replaced by nonphenotypic stem cells.

Interestingly, although mosaic forms of EHK have been described (Paller et al., 1994), a mosaic form of EBS has never been reported. Mosaic forms of EHK probably arise through postzygotic mutations, and the distribution of affected epidermis reflects migration and proliferation of mutant epidermal stem cells (Paller et al., 1994). To explain the absence of mosaic forms of EBS, it is tempting to speculate that when postzygotic mutations occur in K5 or K14, the epidermal stem cells carrying the mutation would have a selective disadvantage and be rapidly displaced by

wild-type stem cells. Consistent with the clinical observations, focal lesions were observed in chimeric EHK mice derived from +/mut^{loxP} ES cells (Arin et al., 2001), but not in chimeric +/mtK14^{loxP} mice.

Our inducible transgenic mouse model (mtK14^{neo}/CrePR1) allows focal induction of EBS phenotypes while the mice remain viable. Thus, it is ideally suited to test gene therapy approaches for EBS-DM in vivo. Chimeric RNA–DNA oligonucleotides could be used to correct the point mutation in the mutant K14 allele through homologous recombination and mismatch repair (Cole-Strauss et al., 1996; Alexeev et al., 2000). Alternatively, the fact that +/mtK14^{neo} mice expressed low levels of mutant K14 but had morphologically normal and functional skin suggests that the EBS phenotype may be corrected by increasing the ratio of wild-type versus mutant K14. This could be achieved by either increasing the expression of the wild-type K14 or partial suppression of the mutant K14 allele.

We are grateful to Richard R. Behringer and Yuji Mishina for the PGK-neobpA plasmid and Steve O'Gorman for the CMV-Cre plasmid. We would like to thank Richard R. Behringer, Yuji Mishina, Benny Chan, Guangbin Luo, and members of the Roop laboratory, especially Peter J. Koch, for their suggestions during the development of this project and Donna Wang and Olga Shuhatovich for technical assistance. We thank Francisco DeMayo for ES cell injections, Hank P. Adams for electron microscopy, and Craig Allred for use of the PixCell I LCM equipment. T. Cao would like to thank Anika J. and Athula H. Wikramanayake for their support.

This work was supported by grants AR62228 from the National Institutes of Health and the Dystrophic Epidermolysis Bullosa Research Association of America to D.R. Roop.

Submitted: 23 October 2000
Revised: 22 December 2000
Accepted: 29 December 2000

References

Alexeev, V., O. Igoucheva, A. Domashenko, G. Cotsarelis, and K. Yoon. 2000. Localized in vivo genotypic and phenotypic correction of the albino mutation in skin by RNA-DNA oligonucleotide. *Nat. Biotechnol.* 18:43–47.

Anton-Lamprecht, I., and U.W. Schnyder. 1982. Epidermolysis bullosa herpetiformis Dowling-Meara. Report of a case and pathomorphogenesis. *Dermatologica.* 164:221–235.

Arin, M.J., M.A. Longley, X.-J. Wang, and D.R. Roop. 2001. Focal activation of a mutant allele defines the role of stem cells in mosaic skin disorders. *J. Cell Biol.* 152:645–649.

Berton, T.R., X.J. Wang, Z. Zhou, C. Kellendonk, G. Schutz, S. Tsai, and D.R. Roop. 2000. Characterization of an inducible, epidermal-specific knockout system: differential expression of lacZ in different Cre reporter mouse strains. *Genesis.* 26:160–161.

Chan, Y., I. Anton-Lamprecht, Q.C. Yu, A. Jackel, B. Zabel, J.P. Ernst, and E. Fuchs. 1994. A human keratin 14 "knockout": the absence of K14 leads to severe epidermolysis bullosa simplex and a function for an intermediate filament protein. *Genes Dev.* 8:2574–2587.

Chen, H., J.M. Bonifas, K. Matsumura, S. Ikeda, W.A. Leyden, and E.H. Epstein, Jr. 1995. Keratin 14 gene mutations in patients with epidermolysis bullosa simplex. *J. Invest. Dermatol.* 105:629–632.

Cole-Strauss, A., K. Yoon, Y. Xiang, B.C. Byrne, M.C. Rice, J. Gryn, W.K. Holloman, and E.B. Kmiec. 1996. Correction of the mutation responsible for sickle cell anemia by an RNA-DNA oligonucleotide. *Science.* 273:1386–1389.

Coulombe, P.A. 1993. The cellular and molecular biology of keratins: beginning a new era. *Curr. Opin. Cell Biol.* 5:17–29.

Dowling, G.B., and R.H. Meara. 1954. Epidermolysis bullosa dermatitis herpetiformis. *Br. J. Dermatol.* 66:139–143.

Hatzfeld, M., and K. Weber. 1990. The coiled coil of in vitro assembled keratin filaments is a heterodimer of type I and II keratins: use of site-specific mutagenesis and recombinant protein expression. *J. Cell Biol.* 110:1199–1210.

Jonkman, M.F., K. Heeres, H.H. Pas, M.J. van Luyn, J.D. Elema, L.D. Corden, F.J. Smith, W.H. McLean, F.C. Ramaekers, M. Burton, and H. Scheffer. 1996. Effects of keratin 14 ablation on the clinical and cellular phenotype in a kindred with recessive epidermolysis bullosa simplex. *J. Invest. Dermatol.* 107:764–769.

Kellendonk, C., F. Tronche, A.P. Monaghan, P.O. Angrand, F. Stewart, and G. Schutz. 1996. Regulation of Cre recombinase activity by the synthetic steroid RU 486. *Nucleic Acids Res.* 24:1404–1411.

Letai, A., P.A. Coulombe, M.B. McCormick, Q.C. Yu, E. Hutton, and E. Fuchs. 1993. Disease severity correlates with position of keratin point mutations in patients with epidermolysis bullosa simplex. *Proc. Natl. Acad. Sci. USA.* 90:3197–3201.

Lloyd, C., Q.C. Yu, J. Cheng, K. Turksen, L. Degenstein, E. Hutton, and E. Fuchs. 1995. The basal keratin network of stratified squamous epithelia: defining K15 function in the absence of K14. *J. Cell Biol.* 129:1329–1344.

Marinkovich, M.P., G.S. Herron, P.A. Khavari, and E.A. Bauer. 1999. Hereditary epidermolysis bullosa. *In* Fitzpatrick's dermatology in general medicine. I.M. Freedberg, A.Z. Eisen, K. Wolff, K.F. Austen, L.A. Goldsmith, S.I. Katz, and T.B. Fitzpatrick, editors. McGraw-Hill Co., New York. 690–702.

McGrath, J.A., A. Ishida-Yamamoto, M.J. Tidman, A.H. Heagerty, O.M. Schofield, and R.A. Eady. 1992. Epidermolysis bullosa simplex (Dowling-Meara). A clinicopathological review. *Br. J. Dermatol.* 126:421–430.

Moll, R., W.W. Franke, D.L. Schiller, B. Geiger, and R. Krepler. 1982. The catalog of human cytokeratins: patterns of expression in normal epithelia, tumors and cultured cells. *Cell.* 31:11–24.

Morley, S.M., S.R. Dundas, J.L. James, T. Gupta, R.A. Brown, C.J. Sexton, H.A. Navsaria, I.M. Leigh, and E.B. Lane. 1995. Temperature sensitivity of the keratin cytoskeleton and delayed spreading of keratinocyte lines derived from EBS patients. *J. Cell Sci.* 108:3463–3471.

Paller, A.S., A.J. Syder, Y.M. Chan, Q.C. Yu, E. Hutton, G. Tadini, and E. Fuchs. 1994. Genetic and clinical mosaicism in a type of epidermal nevus. *N. Engl. J. Med.* 331:1408–1415.

Potten, C.S., R. Saffhill, and H.I. Maibach. 1987. Measurement of the transit time for cells through the epidermis and stratum corneum of the mouse and guinea-pig. *Cell Tissue Kinet.* 20:461–472.

Quinlan, R.A., D.L. Schiller, M. Hatzfeld, T. Achtstatter, R. Moll, J.L. Jorcano, T.M. Magin, and W.W. Franke. 1985. Patterns of expression and organization of cytokeratin intermediate filaments. *Ann. NY Acad. Sci.* 455:282–306.

Rothnagel, J.A., and D.R. Roop. 1995. Analysis, diagnosis, and molecular genetics of keratin disorders. *Current Opininon in Dermatology.* 1995:211–218.

Rugg, E.L., W.H. McLean, E.B. Lane, R. Pitera, J.R. McMillan, P.J. Dopping-Hepenstal, H.A. Navsaria, I.M. Leigh, and R.A. Eady. 1994. A functional "knockout" of human keratin 14. *Genes Dev.* 8:2563–2573.

Steinert, P.M. 1990. The two-chain coiled-coil molecule of native epidermal keratin intermediate filaments is a type I-type II heterodimer. *J. Biol. Chem.* 265:8766–8774.

Steinert, P.M., and D.R. Roop. 1988. Molecular and cellular biology of intermediate filaments. *Annu. Rev. Biochem.* 57:593–625.

Vassar, R., P.A. Coulombe, L. Degenstein, K. Albers, and E. Fuchs. 1991. Mutant keratin expression in transgenic mice causes marked abnormalities resembling a human genetic skin disease. *Cell.* 64:365–380.

Wang, X.J., D.A. Greenhalgh, X.R. Lu, J.R. Bickenbach, and D.R. Roop. 1995. TGF alpha and v-fos cooperation in transgenic mouse epidermis induces aberrant keratinocyte differentiation and stable, autonomous papillomas. *Oncogene.* 10:279–289.

Wojcik, S.M., D.S. Bundman, and D.R. Roop. 2000. Delayed wound healing in keratin 6a knockout mice. *Mol. Cell Biol.* 20:5248–5255.